JMEPEG (2006) 15:474-483
DOI: 10.1361/105994906X117332

1059-9495/$19.00

Fuel Cell and Hydrogen Economy

Ramana G. Reddy

(Submitted January 16, 2006; in revised form May 21, 2006)

This article reviews some of the recent developments in the materials, design, and concepts for bipolar/end plates in the polymer electrolyte membrane fuel cell stack. Experimental results for the use of iron- and copper-based alloys for bipolar plate as an alternative to the expensive conventionally used graphite material are presented. The developments of the models for optimizing the design parameters in the gas flow-field of these plates are discussed. Based on these simulations results, some of the new concepts for these plates were urbanized. These include: use of metal foam in the gas flow-field, and corrugated thin sheet bipolar/end plate. Experimental results with these new concepts are presented and will be compared with the model-predicted results. Applications of these new concepts in the development of commercial fuel cell stacks in the era of hydrogen economy are discussed.

Keywords bipolar plates, corrugated sheets, metal foams, modeling, polymer electrolyte membrane fuel cell

1. Introduction

Successful application of fuel cell technology is the key for a sustainable hydrogen economy. The application of fuel cell technology to portable power systems is motivated by several factors including high power density, high energy-to-weight ratio, and, more importantly, an environmentally benign process. However, the miniaturization of fuel cells for portable power applications is not simply a matter of reducing physical dimensions but of making use of new designs and manufacturing processes for micro and macro components. This puts a limitation on the materials and processes used for making such components. The widespread commercialization of the technology has still not been made possible due to the high costs associated with the fuel cell components. One such component in the fuel cell stack is the bipolar/end plate. These are one of the costliest components in the fuel cell stack and account for >80% of the total weight of the stack (Ref 1). The working of polymer electrolyte membrane fuel cell (PEMFC) is similar to that of other fuel cells. Generally, hydrogen (H_2) is fed to the porous anode as fuel and an oxidant, either oxygen (O_2) or oxygen-enriched air, is passed on the cathode surface. The reactions that take place are as follows (Ref 2, 3).

$$\text{At anode} - \quad H_2 \rightarrow 2H^+ + 2e^- \qquad E^0 = 0 \text{ V}$$

$$\text{At cathode} - \quad \tfrac{1}{2}O_2 + 2H^+ + 2e^- \rightarrow H_2O \qquad E^0 = 1.229 \text{ V}$$

The overall reaction is thus:

$$H_2 + \tfrac{1}{2}O_2 \rightarrow H_2O \qquad E^0 = 1.229 \text{ V}$$

This paper was presented at the ASM Materials Solutions Conference & Show held October 18-21, 2004 in Columbus, OH.

Ramana G. Reddy, ACIPCO Professor, Interim Department Head & Associate Director of Centre for Green Manufacturing, Department of Metallurgical and Materials Engineering, The University of Alabama, Tuscaloosa, AL 35487. Contact e-mail: rreddy@coe.eng.ua.edu.

Figure 1 shows the detailed working of the PEMFC. The water thus produced can be reused by recirculation to keep the membrane hydrated.

2. Fuel Cell Research at The University of Alabama

The fuel cell research at The University of Alabama started in year 1999. The research areas are multidisciplinary, and various department are working together to develop a system integration module for PEMFC, direct methanol fuel cell (DMFC), and solid oxide fuel cell (SOFC). The research areas includes bipolar plates, end plates, membranes, electrodes, catalysts, controls for fuel cell systems, and the effect of vibrations on cell stack components. The metallurgical and materials engineering department at The University of Alabama is currently working on the development of new materials, designs, and modeling of bipolar and end plates (Ref 4-6). Fuel cell research in DMFCs is mainly focused on the design of and material modification for bipolar and end plates. Ongoing research is for the modeling and optimization of flow fields. The other aspects of the development of electrode and membrane materials are also ongoing. The research is also active in development of interconnect materials for SOFC. This paper discusses some of the research finding pertaining to PEMFC bipolar/end plates.

3. Development of Bipolar/End Plate Materials for Polymer Electrolyte Membrane Fuel Cell

3.1 Selection of Material

This is the first step in the development of bipolar/end plate material. Material selection is a very critical step where lots of possible materials are considered. The short-listed materials were then compared, and some of them were eliminated on the basis of various properties. The materials that were considered fall into four major groups (Ref 7): metals and alloys; composites; conducting polymers; and ceramics. Semiconductors were not considered due to their cost and lack of corrosion resistance. As discussed above, although composites and con-

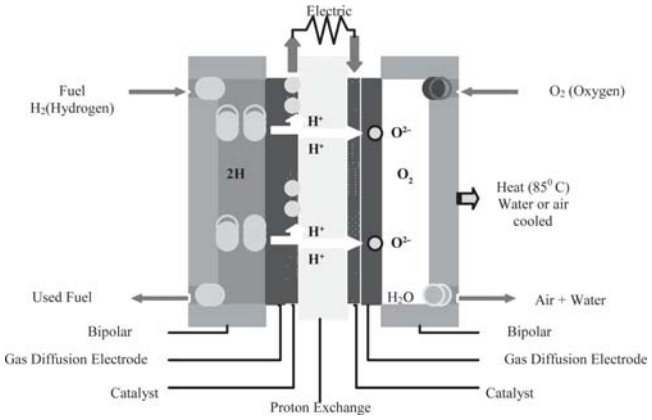

Fig. 1 Working of the PEMFC

Table 1 Comparison of SS-316 and C-17200 with graphite

Property	Graphite	SS-316	C-17200
Cost, $/kg	75	7	12
Density, g/cc	2.25	8.02	8.25
Thickness of bipolar plate for same weight, mm	2.50-4.00	0.16	0.16
Thermal conductivity, J/cm · °C · s	0.24	0.16	1.3
Electrical resistivity, Ω-cm × 10^{-6}	6000	73	46.2
Permeability for hydrogen across the plates, cm^3/cm^2-s	10^{-2}-10^{-6}	$<10^{-12}$	$<10^{-12}$
Modulus of elasticity, MPa	4800	193,000	18,500
Corrosion current, mA/cm^2	<0.01	<0.026	<0.025

ducting polymers were used they were rejected on the basis of their cost and lower ease of manufacturing. Most of the alloy systems have good conductivity and strength, and low cost. Metals and alloys are promising in each and every aspect considered. So, the focus of this research was on testing of some of the alloy systems. After reviewing the materials on the basis of their properties, SS-316 and C-17200 alloys were selected as a candidate material for PEMFC bipolar plates. The properties of these alloys are compared with graphite, which is a commercially used bipolar plate material, and are given in Table 1.

After finishing with the selection of the material, an extensive corrosion study of the C-17200 alloy was carried out in a simulated fuel cell environment (Ref 8). The details of the corrosion testing are not included in this article. The corrosion testing was followed by the modeling to study the optimization of the flow field.

3.2 Modeling of Flow Fields

Among the different types of fuel cells that exist, the PEMFC-type cell is seen as a system of choice for automobile applications due to its environmentally friendly nature and ability to deliver high power density while operating at lower temperatures (Ref 2). With such a great progress in fuel cell technology taking place in the last decade, one of the main hindrances in the onset of the fuel cell commercialization program is the high cost of the fuel cell system (Ref 9). Therefore, the main focus for fuel cell developers is to improve the performance of different components of the fuel cell stack and

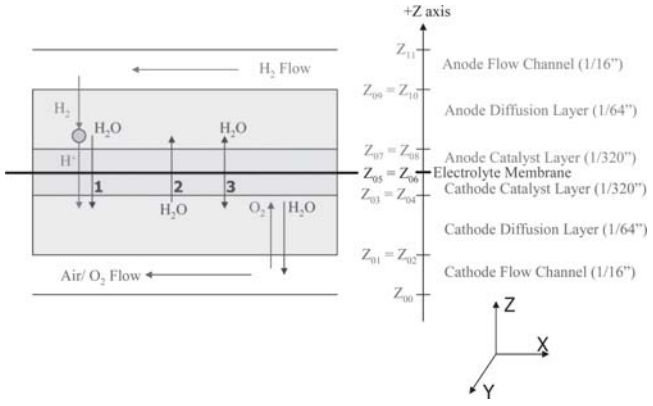

Fig. 2 Schematic of the PEMFC cross section showing different zones and species transport across the zones. The net water flux is the sum of: (1) electro-osmotic effect; (2) diffusion effect; and (3) permeability effect

thereby increase the cell efficiency. This can be achieved by optimizing the operating parameters and selecting newer materials with better performance. But the complex nature of interlinking between different components makes the optimization a challenging task. However, with the advent of advanced modeling tools and the computational environment, enhanced system integration and optimization for the fuel cell stack is becoming a reality. Several models have been developed in the past for different components in the fuel cell system (Ref 10-18). The use of such models will enhance our understanding and development of efficient fuel cell systems.

3.3 Single-Cell Model

The single-cell stack uses SS-316 bipolar/end plates with a multiparallel flow-field design. The model focuses on predicting the effect of operating parameters like humidification level, temperature, and pressure. Simulations were carried out to study the effect of these parameters on cell performance. The model will help in obtaining the optimum operating parameters without the need to do many costly experiments. The detailed stepwise development of the model is discussed below.

3.4 Problem Domain

The simulation domain consists of bipolar/end plate flow-field channels, anode and cathode diffusion, and a catalyst layer, on each side of the membrane. Each of the layers is marked as a separate zone in Fig. 2. The cathode and anode flow channels were imprinted onto the bipolar/end plates. The diffusion layers were essentially the electrodes made with porous carbon cloth.

These layers help to diffuse the reactant gases from the bipolar/end plate flow channels onto the reaction catalyst layer on each side of the membrane. The pressure drop of the reactants due to the porous layer was also taken into consideration in this modeling work. It was assumed that these layers have an isotropic permeability and that the value is 10^{-12} m^2 (Ref 11). The catalyst layer is where all the electrochemical reactions take place. Four species (i.e., hydrogen, oxygen, nitrogen, and water vapor) were considered in this modeling work. The model works by tracking the fluxes of all the reactants along with the byproduct water that is formed due to the electrochemical reaction. Consider, for example, the flux for hydro-

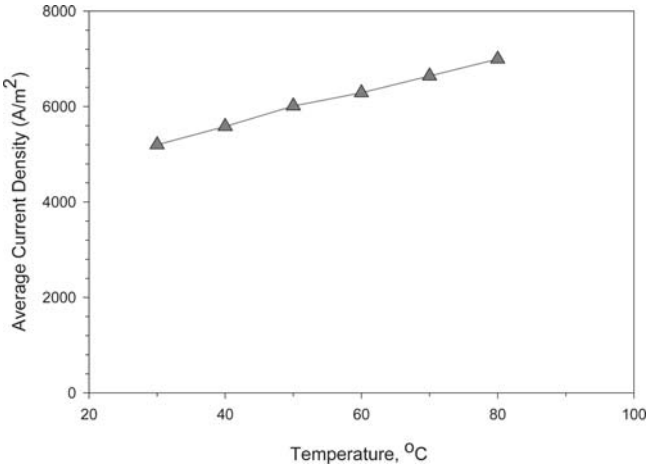

Fig. 3 Single-cell model simulations at different temperatures ranging from 30 to 80 °C

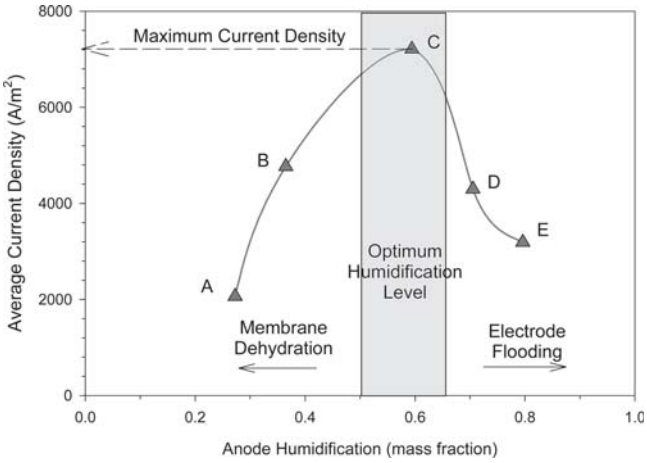

Fig. 4 Simulation results for the variation of average current density as a function of the humidification level of the reactant gases

gen species. The hydrogen from the anode flow channel is transported through the anode diffusion layer toward the anode catalyst layer. The catalyst action dissociated the hydrogen molecule to protons and electrons according to the reaction $H_2 \rightarrow 2H^+ + 2e^-$. The protons generated above will transfer through the membrane (protonic conductor) onto the cathode side, wherein they combine with oxygen to generate water. So, there is a consumption of hydrogen and oxygen species on the anode and cathode sides, respectively, and a generation of water species on the cathode side. Similarly, other species are tracked in the domain. The assumptions, solution strategy, and governing equations have already been discussed separately in another article (Ref 4).

3.4.1 Simulations. Simulations were done for different operating conditions (i.e., humidification, temperature, and pressure). The idea behind doing these simulations was to find the optimum operating parameters, so that the cell stack could be run with those parameters. Operating at these parameters will yield the maximum performance in terms of the output and life of the fuel cell system. It should be noted that while doing a simulation on one parameter, all other parameters were kept constant. For example, to study the effect of humidification level, only the composition of the reactants was changed, and all other parameters, like temperature, pressure, and operating voltage, remained constant.

3.5 Effect of Humidification

Simulations were performed for varying degrees of different humidification levels (content of H_2O in the anode and cathode streams) in the cell stack. The average current density for each case A, B, C, D, and E was 2062, 4767, 7209, 4295, and 3187 A/m^2, respectively. The details of all the results are included in a previously published article (Ref 4).

It is clear from these simulations that humidification level is an important parameter for efficient cell performance. Because the water is produced on the cathode side of the cell, membrane dehydration is highly unlikely on this side. The cell performance is then entirely dictated by the water content at the anode side. The results obtained above can be represented in a more convincing way in Fig. 3. Five humidification cases are represented here, and the graph shows a peak kind of performance. On each side of the peak, the performance of the fuel cell decreases. Toward the left, the performance is low due to membrane dehydration (i.e., low ionic transfer coefficient), and on the right side the performance drops due to flooding of the electrode pores. So, the optimum humidification level corresponds to the peak of the curve. It may be noted here that in practical systems it may be difficult to maintain a precise level of humidification.

3.6 Effect of Temperature

Simulations were performed in a temperature range of 30 to 80 °C in steps of 10 °C. The pressure for these simulations was kept constant at 240 kPa. The results are plotted in Fig. 4. As expected, an increase in performance is observed. The linear fit of the simulated data yields the equation:

$$CD = 35.5 \times T + 4165 \quad (R^2 = 0.9973)$$

where CD is the current density in amperes per square meter, and T is the temperature in degrees centigrade It should be noticed here that this equation is typical for our single-cell stack in particular, and may vary slightly in other stack designs and with other fuel cell materials.

The equation shows a direct relationship between temperature and current density in the cell for a fixed operating voltage of 0.6 V. The graph shows a constant increase in current density with temperature. This is due to the reduced internal resistance of the cell, the reduced mass transport limitations, and the enhanced kinetics of the electrochemical reactions as the temperature is increased. Also, when the fuel cell stack is operated on the reformer feed at high temperature, it reduces the chemisorption of CO on the catalysts. This enables the fuel cell to be operated with some level of CO contaminant without catalyst poisoning. The improvement in cell performance with increase in cell temperature is limited by the high vapor pressure of water in the electrolyte membrane. This is due to the dehydration of the electrolyte membrane and consequently to the reduction in the protonic conductivity as the temperature is increased. The choice of optimum operating parameters in such cases is, however, complex and depends on the performance of the fuel cell materials. Typically, the performance of the electrolyte membrane dictates the choice of the optimum operating temperatures in the cell.

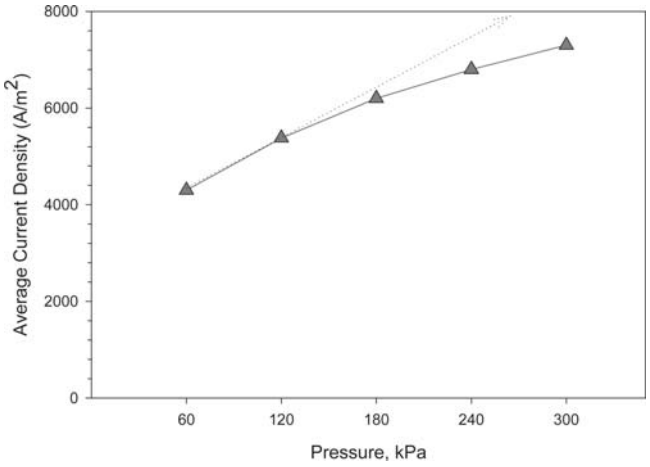

Fig. 5 Single-cell model simulations at different pressures ranging from 60 to 300 kPa

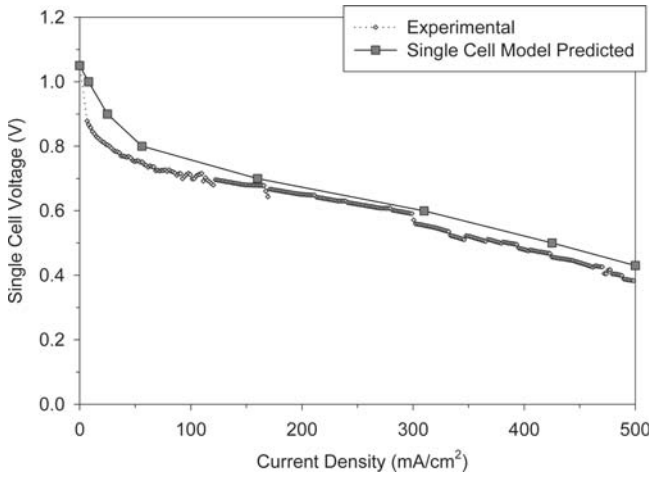

Fig. 6 Validation of the single-cell model with experimental data

3.7 Effect of Pressure

Simulations similar to that for temperature were performed for pressures ranging from 60 to 300 kPa in steps of 60 kPa. The temperature and operating voltage for these simulations was kept constant at 80 °C and 0.6 V, respectively. The results are plotted in Fig. 5. The performance increases rapidly in the beginning but slowly levels off as pressure increases. This is due to the reduced rate of gas solubility as the pressure is increased. The choice of optimum operating pressure depends on the type of application. In general, high operating pressures must be avoided in fuel cell operation. High operating pressures unnecessarily add to the cost of pressurization of the reactant gases.

3.8 Model Validation

The unified single-cell model results for current density predictions were compared with the experimental data obtained using a single-cell PEMFC stack. Bipolar/end plates were made of SS-316 with multi-parallel flow-field (MPFF) design and rectangular cross-section channels. Experiments were run with simulated H_2 and H_2O flow through the anode compartment, and with simulated O_2 and H_2O on the cathode side. Gas inlet temperature and pressure were maintained at 350 K and 240 kPa, respectively.

Simulations were performed at voltages ranging from 1.0 to 0.4 V in steps of 0.1 V using the thermodynamic and membrane properties (Ref 4, 6). The simulated results of cell voltage as a function of current density for a single-cell stack are compared with our experimental data, as shown in Fig. 6. A good agreement between the experimental and simulated data was obtained. The discrepancy between model-predicted and experimental data at low current densities or at higher voltages (the activation polarization range) may be due to the changes in temperature and pressure in the stack. In the experimental system, these were not measured, and temperature and pressure was assumed to be the same as that of the inlet gases. The fact that the experimental results are lower than the predicted results indicates that the experimental flow-field-membrane electrode assembly (MEA) system could have lower temperatures and pressures than 350 K and 240 kPa, respectively. This unified model can now be used to study the effect of different operating variables (i.e., humidification, temperature, and pressure) and to predict the fuel cell performance. However, this model is valid only for the MPFF design of the bipolar/end plates and defined experimental conditions.

3.9 Gas Flow-Field Design

The gas flow field is one of the most important design parameters that directly affect cell performance. Several models have been developed for the optimization of the electrochemical kinetics of the process. However, little attention has been focused on the optimization of the flow-field design in the bipolar/end plates of the fuel cell stack (Ref 10, 19). This work concentrates on the effect of the flow-field design on the steady-state and the transient behaviors of the fuel cell. Several flow-field designs (i.e., serpentine, parallel, multiparallel, and discontinuous) were studied for the steady-state and transient performances of the fuel cell.

3.10 Model Development

The current model is a three-dimensional, single-phase, transient, isothermal, numerical mass-transfer unified model for PEMFCs. The steady-state performance is just a special case where all the time-dependent terms in the governing transport equations would be nullified. Essentially, this model is an extension of the single-cell model described above. The numerical predictions of the voltage were made for changing load (current) levels. The transient behavior was studied for different flow-field designs (i.e., serpentine, parallel, multiparallel, and discontinuous) in the bipolar/end plates of the fuel cell. Also, the steady-state performance was calculated for each of the designs, and the results were compared. The overall performance of the flow-field design was judged based on the steady-state and transient behaviors of the fuel cell. This would help in finding the best possible flow-field design for the bipolar/end plates of the fuel cell. The details about the assumptions, governing equations, and solution strategies have been published elsewhere (Ref 4, 6).

3.10.1 Simulations. Simulations were performed for different flow-field designs in the bipolar/end plates of the PEMFC. The temperatures and pressures for all of the simulations were kept constant at 350 K and 202 kPa, respectively. Reactant gases were externally humidified. On the cathode side, humidified air consisting of 21 mass% O_2, 70.5 mass%

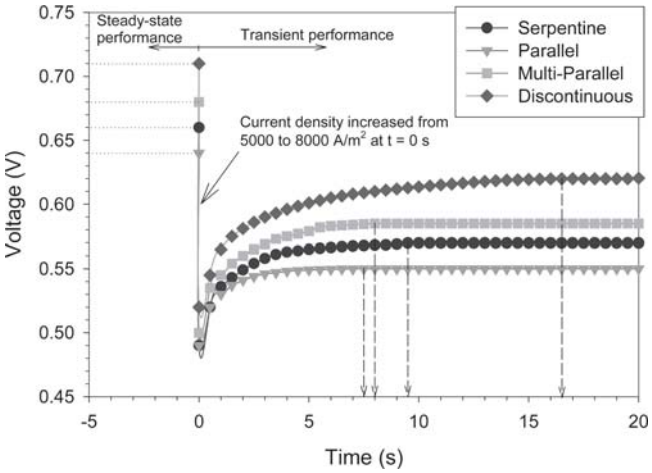

Fig. 7 Steady-state and transient performance for a single-cell PEMFC stack using different flow-field designs in the bipolar/end plates

N_2, and 8.5 mass% H_2O vapor was used. The anode side reactant gas consisted of 40 mass% H_2 and 60 mass% H_2O vapor. The velocity inlets for the cathode and anode sides were 5.0 and 2.5 m/s, respectively.

The steady-state results were first obtained by deselecting the transient option from the Fluent software (Fluent Inc., Lebanon, NH). Deselecting essentially removes all of the time-dependent terms from the transport equations. The current density for these simulations was fixed at 5000 A/m^2. The simulated voltages for serpentine, parallel, multiparallel, and discontinuous designs were 0.66, 0.64, 0.68, and 0.71 V, respectively. These are marked by dotted lines in the steady-state region of Fig. 7. From this, the authors concluded that the discontinuous type of flow-field design will perform better than the other three designs. This is because the discontinuity of the channels forces the gas into the diffusion layer, thereby making the transfer of the reactant gases in the gas diffusion layer from diffusion to diffusion plus forced convection type. This increases the effective pressure of the reaction species at the reaction interface. These findings are consistent with those of Watkins et al. (Ref 19), who proposed the design as a solution to the problem of increased gas diffusion. The transient response of the PEMFCS was studied by changing the load level (current) from 5000 to 8000 A/m^2 instantaneously. The sudden load change was made at time $t = 0$ s. It was assumed that the fuel cell has a steady state at all times, $t < 0$ s. The simulated voltage for the transient region is shown in Fig. 7. Initially, when the load level is increased, the voltage suddenly drops, and then levels off to a value slightly higher than the dropped value. The time to level off was measured from the time when the load level was suddenly increased ($t = 0$ s) to the time when the change in voltage was <0.1 mV. The times for the transient responses for the serpentine, parallel, multiparallel, and discontinuous types of flow designs were 9.5, 7.5, 8.0, and 16.5 s, respectively. It was seen that the transient performance was highest for the parallel type of design and lowest for the discontinuous type of design.

As discussed above, the discontinuous type of design gave the maximum steady-state performance but the lowest transient performance. On the other hand, the parallel design gave the lowest steady-state performance but the highest transient performance; the multiparallel type of flow-field design gave reasonably good values for both steady-state and transient performance. So, with such flow-field designs in the bipolar/end plates the overall performance of the fuel cell can be increased.

Also, it is worth mentioning that the use of the design also depends on the application. If the fuel cell is used for stationary applications where the steady-state response is more important than the transient response, the discontinuous type of flow-field design will be a better choice. However, if the fuel cell is used for automobile applications, where the transient response is as important as the steady-state performance, it would be wise to use the multiparallel type of flow-field design.

Also, it may be noted that the difference in voltage transient response values for different flow-field designs were on the order of 0.1 V, which may appear to be insignificant. These values should be used as a caution, because this depicts the voltage variation in one cell only. In commercial cell stacks (approximately $\geq$100 cells), the voltage variations from all cells would add up, resulting in an appreciable level of transient voltage drop. The present model in further studies would be extended to study the transient characteristics for the large fuel cell stacks. The use of such models will help in the optimization of the design process for the gas flow-field and will give fuel cell developers a scope of further improvements of the fuel cell technology.

3.11 Optimization of Channel Dimensions and Shape

The efficiency of the fuel cell depends on the kinetics of the electrochemical process and the performance of the components. However, as discussed in the previous sections, little attention is being focused on the design dimensions for the fuel cell, typically those of the flow field of the bipolar/end plate. This work therefore concentrates on studying the effects of the dimensions and shape of the channels in the gas flow field (Ref 4). This would help to better understand some of the design consider ations for the bipolar/end plates and will give fuel cell developers a scope of further improvement of the fuel cell technology.

The PEMFC model described here was developed to study the effect of the channel dimensions and shapes in the flow field of the bipolar/end plates. Consequently, to avoid complexities, a half-cell model for the anode side of the fuel cell was developed. The problem domain for the half-cell PEMFC model consists of three different zones: flow-field channels (serpentine design), which are imprinted onto the bipolar/end plates; gas diffusion electrodes; and catalyst layers. It was assumed that the fuel was hydrogen on the anode side. The hydrogen gas enters the domain at the gas inlet in the bipolar/end plate. The gas flow field in the bipolar/end plate helps in the distribution of hydrogen reactant gas onto the surface of the electrode. The gas is transported toward the anode electrode via diffusion and convective transfer. The next layer is the catalyst layer, where hydrogen molecules break into protons and electrons.

Rectangular cross-section channels were chosen for studying the effect of channel dimensions. The flow field was chosen to be a single-path serpentine design. Once the optimum channel dimensions have been achieved, the results would be compared with those of other channel shapes. The data and more discussion for this model have been published previously (Ref 4, 6).

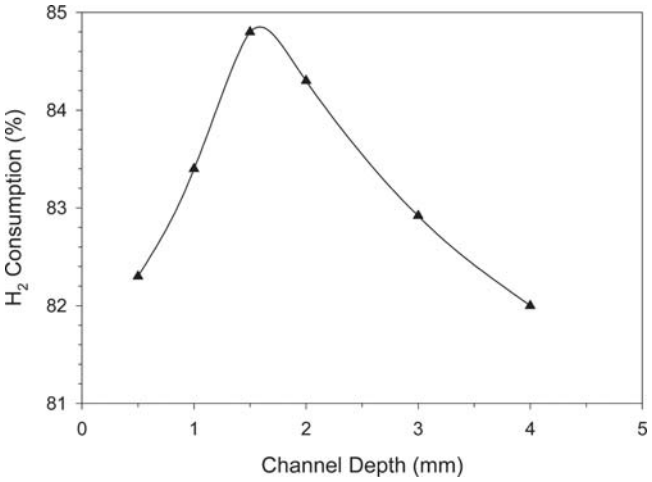

Fig. 8 Effect of channel depth in the flow field of the bipolar/end plate on hydrogen consumption at the anode

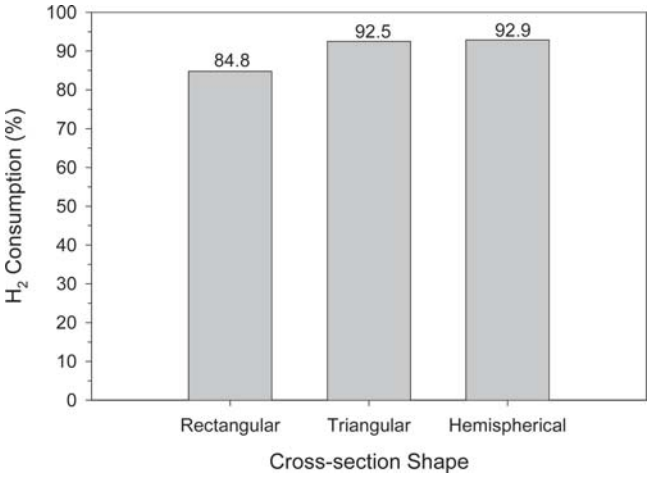

Fig. 9 Effect of the channel cross section on hydrogen consumption in the bipolar/end plate flow field

3.11.1 Simulations. Simulations were performed for different sets of channel dimensions. Three different parameters (channel depth, channel height, and land width) were chosen for study. Each of the parameters was varied from 0.5 to 4.0 mm, resulting in a total of six different dimension cases (i.e., 0.5, 1.0, 1.5 2.0, 3.0, and 4.0 mm). With all of the permutations and combinations among the parameters, we have a total of $6 \times 6 \times 6 = 216$ cases. Hydrogen consumption at the anode was chosen as the parameter to judge the performance of the fuel cell. It may be noted that the higher the hydrogen consumption at the anode, the better the performance of the fuel cell. Simulations corresponding to these 216 cases were performed for different chosen values of λ. We choose four different values of λ corresponding to 5, 10, 15, and 20. The hydrogen consumption for each of these cases came out to be roughly 20, 42, 63 and 83 mass%, respectively. Considering the fact that the practical fuel cell operates at high values of fuel consumption (e.g., 80 mass%), it was decided to choose a value of λ of 20 for the simulations. Further, the simulations performed at low values of λ like 5 or 10 showed little effect on changing the channel dimensions with hydrogen consumption. This was expected, because diffusion mass limitations of hydrogen in areas on ribs (land area) would be small at low reaction rates (with low hydrogen consumption). Figure 8 shows the effect of change in channel depth with hydrogen consumption at the anode with optimum channel width (1.5 mm) and land width (0.5 mm). So, the established optimum dimensions from these simulations were a channel width of 1.5 mm, a land width of 0.5 mm, and a channel depth of 1.5 mm. These results were consistent with those observed by other researchers in their work. Watkins et al. (Ref 19) studied the optimal dimension for bipolar channels on the cathode side of the fuel cell. They claimed the most preferred ranges to be 1.14 to 1.4 mm for channel width, 0.89 to 1.4 mm for land width, and 1.02 to 2.04 mm for channel depth. Based on the results, that hydrogen consumption at the anode increases as land width decreases, it was decided to study cases in which land width can be reduced, close to a value of zero (0^+ mm). However, making such bipolar/end plate gas flow-field channels with very small land width (~0 mm) by a machining or casting process is not practically feasible. Therefore, alternative methods must be looked at to fabricate such designs. One such method that can be used is the corrugated rolling process. However, this method is good only for metal/alloy systems. Keeping in mind that the currently used graphite bipolar/end plates suffer from some disadvantages (e.g., high machining cost and low mechanical properties) (Ref 20, 21) and that much research is focused on the use of metallic bipolar/end plates, it was decided to study these systems. Based on the foregoing discussion, it was decided to model triangular- and hemispheric-shaped cross sections for the flow-field design using the Fluent CFD tool. Using such channels serves our two purposes. First, to achieve close to zero value for land width, and second, to achieve a higher pressure drop, both of which will provide enhanced fuel cell performance.

The simulation results for the triangular- and hemispheric-shaped cross sections are represented in Fig. 9. These results are plotted for optimum channel dimensions, which were obtained for rectangular-shaped cross-section channels. For triangular cross sections, these dimensions are: channel width, 1.5 mm; channel depth, 1.5 mm; land width, 0^+ mm. For hemispherical cross sections, these dimensions are: channel width, 1.5 mm; land width, 0^+ mm. It may be noted that in the case of hemispherical cross sections, by choosing a channel width of 1.5 mm (the diameter of the hemisphere), the channel depth (the radius of the hemisphere) became 0.75 mm.

The bar graph shows the hydrogen consumption at the anode for triangular and hemispherical cross sections, and compares these values to those for rectangular cross sections. The hydrogen consumption for the triangular-shaped cross-section channels was 92.5%, while that for hemispheric-shaped cross-section channels was 92.9%. These values are approximately 9% more than those for rectangular-shaped cross sections (84.8%). So, it is clear that with the use of cross sections other than those of rectangular shape (like triangular and hemispherical shapes), the hydrogen consumption at the anode will be enhanced, which in turn would enhance the fuel cell performance. Taking these calculations as a guideline for developing a different machining technique, a corrugated sheet bipolar plate was proposed.

3.12 Use of Corrugated Sheet Hemispherical Channel Bipolar Plates

As discussed before, the manufacturing of a bipolar plate is very costly due to the critical machining requirement for flow-

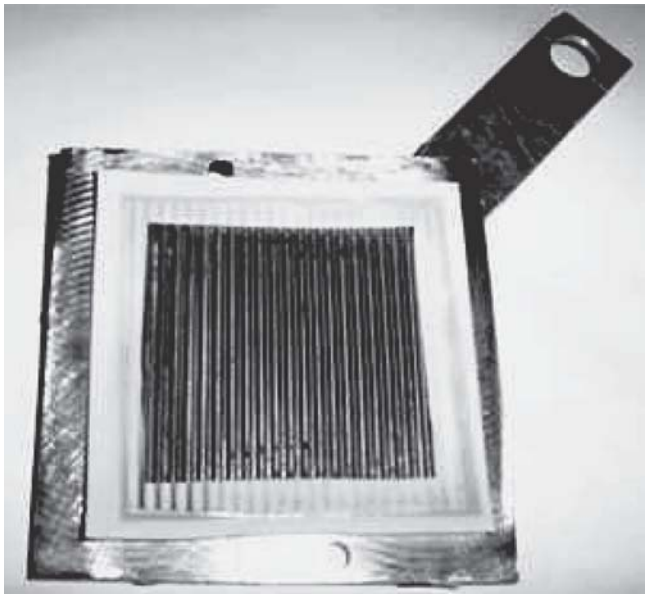

Fig. 10 Corrugated sheet bipolar plate with machined SS-316 supporting plate

field channels (Ref 1). A corrugated sheet bipolar plate manufacturing technique consists of removing machined flow-field channels from bipolar plates with rolled corrugated sheets. Thin sheets of C-17200 alloy were corrugated with a laboratory-type tube wringer. The dimensions of depth, width, and length of corrugation were controlled by roll pressure. The details of manufacturing by this technique are presented in the published literature (Ref 8).

Due to the feeble strength of the sheets, supporting plates of SS-316 were used for the assembly of the single-cell stack. Figure 10 shows the bipolar plate with corrugated sheets. Thin silicon rubber gaskets were used to avoid gas leakage in the cell. The single cell prepared was tested with the fuel cell test station facilities at the University of Alabama. The cell was tested for 250 h at the open circuit potential to observe the degradation of stack potential. The operating conditions were: $T = 60$ °C; $P_{anode} = 15$ psi; $P_{cathode} = 23$ psi; anode flow rate, $Q_a = 29.8$ cm^3/min; and cathode flow rate, $Q_c = 37.5$ cm^3/min.

Figure 11 shows the behavior of the stack potential for 250 h. The stack potential was observed to be constant throughout the duration of test. The average stack potential was calculated to be approximately 0.99 V. The stack was dismantled after the test, and was observed for the corrosion and degradation of the bipolar plate and MEA. Scanning electron microscopy and energy-dispersive spectroscopy analysis revealed no poisoning and corrosion of the MEA and bipolar plates. The use of corrugated sheet not only eliminates the critical machining of the flow-field channels, but also reduces the weight and cost of the bipolar plates (Ref 8). The further testing of such a cell for polarization behavior is underway.

3.13 Effect of Flow-Field Permeability

The current design for the flow field uses the machined rectangular flow channels. Because the flow field helps to distribute the reactant gases on the surface of the electrode, and to remove them with the water byproduct, the dimensions and

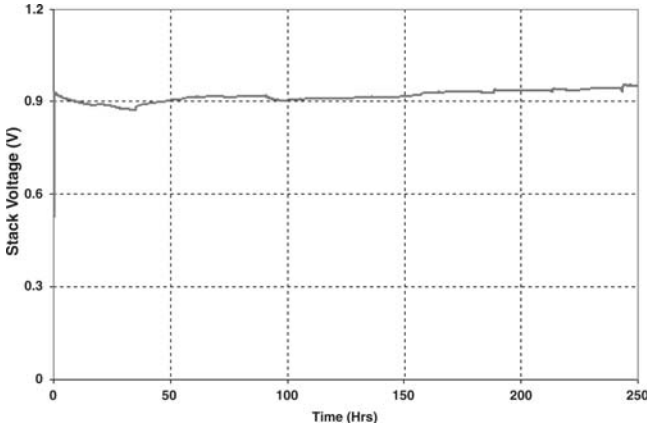

Fig. 11 Long-term stability of a single-cell stack using corrugated sheet bipolar plates

shapes of the channels in the flow field will affect the performance of the fuel cell. It was seen in the previous section that smaller channel dimensions and more channels in the flow field improve the fuel cell performance (Ref 11, 22). For the channel type of flow field, as discussed above, an optimum dimension exists for the channels that would yield maximum performance from the fuel cell (Ref 4). However, in general, the lower the permeability of the flow field, the better would be its performance. Low permeability would result in an increased pressure drop across the flow field. This will make the transfer of reactant gases toward the electrode-membrane reaction interface from a diffusion to forced convection type. However, the permeability value of the flow field can not be decreased beyond 10^{-8} m^2 in the case of channel design due to difficulty in machining thin cross-section channels.

So, there is a need to look for alternative technologies that can produce thin cross-section channels, or will at least give performance equivalent to that of thin channels. The use of foam materials with an open-porous structure in this regard seems promising. Metal foams are a new kind of material that until now have not been characterized properly, but do have some alluring properties. They are light and stiff, have good energy-absorbing characteristics, and good heat transfer properties.

A three-dimensional, steady-state, numerical, mass-transfer unified model for a PEMFC was developed to predict the cell performance. This model is based on the previously developed single-cell model. However, in this case metal foam is present in the gas flow field instead of a channel design. Numerical predictions of current density as a function of the permeability levels of the flow field would be made. This would help in finding the best permeability values for the metal foams that need to be used in the flow field. The model formulation, governing equations, and boundary conditions have been reported in another article (Ref 5).

3.13.1 Simulations. Simulations were performed for different permeability levels of the metal foam flow field. The permeability of the metal foam varied from 10^{-6} to 10^{-12} m^2. Simulations were performed at a temperature and pressure of 350 K and 202 kPa, respectively. Externally humidified reactant gases were used. The anode reactant gas consists of 40 mass% H_2 and 60 mass% H_2O vapor. On the cathode side, the reactant gas was humidified air containing 21 mass% O_2, 70.5 mass% N_2, and 8.5 mass% H_2O vapor. The reactant velocities

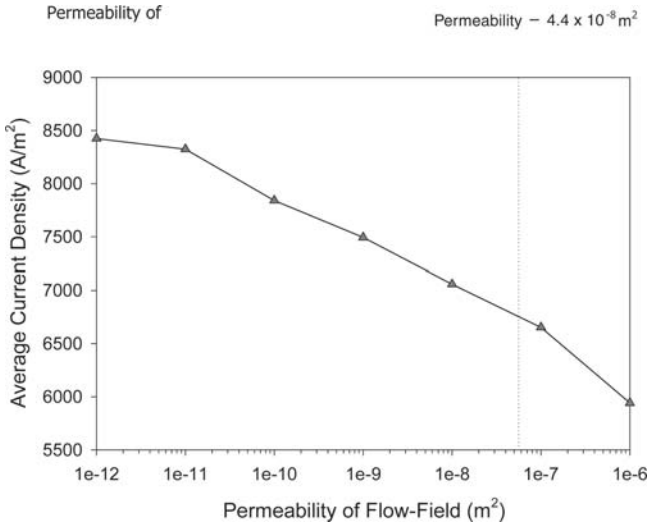

Fig. 12 Variation of average current density with the permeability levels of the metal foam in the flow field of the bipolar/end plates

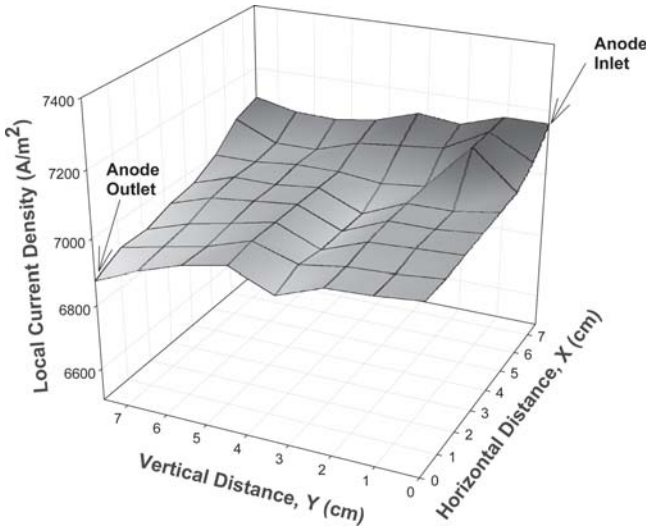

Fig. 13 Distribution of local current density on the electrode-membrane interface for the multiparallel flow-field channel design

at the anode and cathode inlets were fixed at 2.2 and 4.5 m/s, respectively. The cell voltage was fixed at a value of 0.6 V.

Figure 12 shows the variation of the average current density with the permeability of the metal foam used in the flow field of the bipolar/end plate. As was expected, the performance of the cell increased steadily when the permeability was decreased. At very low permeability values, which were comparable to those of the electrodes, the increase in performance started to flatten out. So, it is clear that lower permeability values for the flow field will enhance the fuel cell performance. As already stated, lower values of permeability for the flow field are difficult to achieve in the machined channeled flow field. Consequently, the use of metal foam will be preferred.

To compare the permeability values of metal foam with those of channel design, equivalent permeability for channel design was introduced and was calculated using the expression reported in the literature (Ref 11). It may be noticed that the permeability of the metal foam can be decreased to improve the fuel cell performance. But, on the other hand, it is difficult to reduce the permeability of the channel flow field below a certain level (typically 10^{-8} m^2) due to the difficulty in machining very thin channels.

Also, it is important to note that with the use of metal foam, a more uniform distribution of current density is obtained. Figures 13 and 14 show the distribution of local current density on the electrode-membrane interface for the channel and metal foam types of flow field. It is clearly seen that in the case of metal foam, a more uniform distribution of local current density is observed. Consequently, the use of a metal foam flow field is proposed in the bipolar/end plate. The developed model will give the fuel cell developers a possibility for improving the bipolar/end plates in the fuel cell by switching over to the metal foam flow-field concept.

3.14 Experiments for Different Metal Foam Permeabilities

Figure 15 shows the actual fabricated SS-316 bipolar/end plate with SS-316 metal foam (20 pores per inch [PPI]) in the flow field. The above bipolar/end plates were assembled to

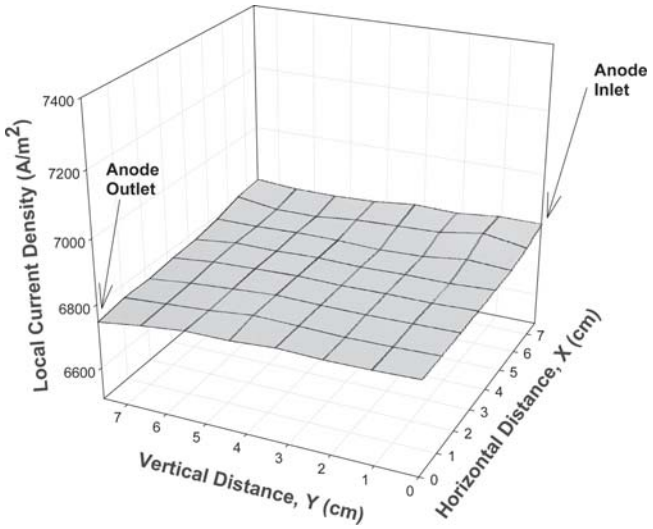

Fig. 14 Distribution of local current density on the electrode- membrane interface with metal foam in the flow field of the bipolar/end plates

form a one-cell fuel cell stack. It may be noted that for one-cell stacks only two end plates and one MEA are required. All experiments were carried out using the fuel cell test station facilities at the University of Alabama. Pure hydrogen and oxygen were used as reactant gases on the anode and cathode sides, respectively. Nitrogen was used as the purging gas. The reactant gases were externally humidified by passing them through a humidification chamber in the gas-controller unit. The operating conditions were $T = 80$ °C; $p = 207$ kPa (both anode and cathode sides); anode flow rate, $Q_a = 150$ cm^3/min + load-based flow (LBF); and cathode flow rate, $Q_c = 80$ cm^3/min + LBF. The polarization curves were obtained by increasing the current output (scan rate 2 mA/s) from the cell and monitoring the cell voltage. Two different types of foam materials were studied: Ni-Cr metal (Fe 8% maximum; C 2% maximum; Cr 30-54%; and Ni balance) foam with 50 PPI; and SS-316 metal foam with 20 PPI. These materials were chosen merely because they were electrically conductive, had good

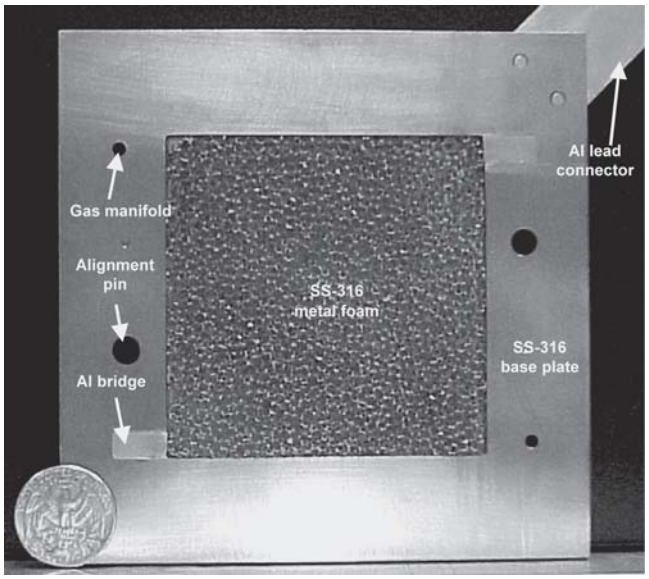

Fig. 15 The PEMFC stack bipolar/end plate with metal foam in the flow-field

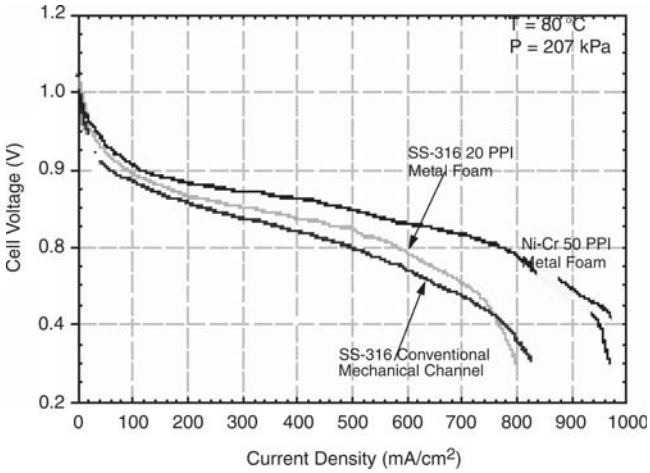

Fig. 16 Polarization curves for different bipolar/end plate concepts

mechanical properties, and were easily available. The aim of this study was to demonstrate the relative performances of metal foams with different permeability values. Polarization studies are typical for any electrochemical system to evaluate its performance. Figure 16 shows the polarization curves for the one-cell PEMFC stack with different bipolar/end-plate concepts.

These curves were obtained by increasing the load level (scan rate 2 mA/s) from the cell and monitoring the cell voltage. As is typical of any electrochemical system, the curve shows a continuous decrease in voltage as the load level is increased. This is due to the polarization losses (activation, ohmic, and concentration), the magnitude of which depends on the amount of current drawn from the cell. Furthermore, it can be seen from Fig. 16 that the performance of Ni-Cr metal foam was highest followed by SS-316 metal foam and conventional multiparallel flow-field channel design.

3.15 Fuel Cell and Hydrogen Economy

The PEMFCs are supposed to be the future of energy-providing systems due to their alluring benefits. They are energy systems that are independent of the price variation of oil prices in the Middle East and so are politically appreciated as well. Apart from the cost, weight, volume, and other technical issues, the safety, cost, and ease of hydrogen generation are the major hurdles for the real application of the fuel cell stack. These problems have different priorities depending on the field of application (Ref 23). The requirements of automobile applications are much more stringent for market penetration, fuel supply, and the servicing of stack parts followed by cost and safety.

When talking about stationary applications, the life times and servicing of cell parts are considered to be the topmost priorities followed by cost and market penetration. Due to the safety norms proposed by the U.S. Department of Energy for the onboard storage of hydrogen (Ref 23), researchers are concentrating on the onboard production of hydrogen. Also, the supply of hydrogen from compressed hydrogen cylinders, liquefied hydrogen cylinders, and gasoline by using fuel reformers are currently active areas of interest for research by some researchers and companies (Ref 24). The implementation of the fuel cell technology for commercial application can be expected when some of these issues have been addressed.

Acknowledgments

Author is thankful for the financial support provided by the U.S. Department of Energy, the U.S. Department of Transportation, and the Center for Advanced Vehicle Technology. I also thank Dr. D. Mantha, Mr. V. Vaibhav, Mr. B. Padhy, and Mr. Y. Lu for their help in the preparation of this article.

References

1. A.S. Woodman, E.B. Anderson, K.D. Jayne, and M.C. Kimble, "Light-Weight and Corrosion Resistant Metal Bipolar Plates for PEM Fuel Cells," Paper 1999-01-2614 presented at Society of Automotive Engineers, p 1-8
2. EG&G Services, Parsons, Inc., U.S. Department of Energy Office of Fossil Energy, and National Energy Technology Laboratory, *Fuel Cell Handbook,* 5th ed., EG&G Services, Parsons, Inc., U.S. Department of Energy Office of Fossil Energy, National Energy Technology Laboratory, 2000, p 1.1-1.37, 2.4-2.8, 2.9-2.16, 10.35-10.37
3. J. Larminie and A. Dicks, *Fuel Cell Systems Explained,* John Wiley & Sons, Ltd., 2000, p 1-108, 181-228
4. A. Kumar and R.G. Reddy, Effect of Channel Dimensions and Shape in the Flow-Field Distributor on the Performance of the Polymer Electrolyte Membrane Fuel Cells, *J. Power Sources,* 2003, **113,** p 11-18
5. A. Kumar and R.G. Reddy, Modeling of a Polymer Electrolyte Membrane Fuel Cell with Metal Foam in the Flow-Field of the Bipolar/End Plates, *J. Power Sources,* 2003, **114,** p 54-62
6. A. Kumar and R.G. Reddy, Materials and Design Development for Bipolar/End Plate in Fuel Cells, *J. Power Sources,* 2004, **129,** p 62-67
7. B.E. Tyler, Wrought Copper and Copper Alloy Products, p. 241-264; P. Robinson, Properties of Wrought Coppers and Copper Alloys, p 265-345; Properties and Sections: Nonferrous Alloys and Special-Purpose Materials, Vol 2, *ASM Handbook,* ASM International, 2000
8. V.V. Nikam, "Copper Alloy Bipolar/End Plates in Polymer Membrane Fuel Cell," M.S. Thesis, The University of Alabama, 2004
9. NECAR 4 The Alternative, Report, Stuttgart: Daimler Chrysler, Corporate Communications: 1999
10. E. Hontanon, M.J. Escudero, C. Bautista, P.L. García-Ybarra, and L. Daza, Optimization of Flow-Field in Polymer Electrolyte Membrane Fuel Cells Using Computational Fluid Dynamics Technique, *J. Power Sources,* 2001, **86,** p 363-368
11. S. Dutta, S. Shimpalee, and J.W. Van Zee, Numerical Prediction of

Mass-Exchange Between Cathode and Anode Channels in a PEM Fuel Cell, *Int. J. Heat Mass Transfer,* 2001, **44,** p 2029-2042
12. J.S. Yi and T.V. Nguyen, An Along-the Channel Model for Proton Exchange Membrane Fuel Cells, *J. Electrochem. Soc.,* 1998, **145,** p 1149-1159
13. T.E. Springer, M.S. Wilson, and S. Gottesfeld, Modeling and Experimental Diagnostics in Polymer Electrolyte Fuel Cells, *J. Electrochem. Soc.,* 1993, **140,** p 3513-3526
14. G. Maggio, V. Recupero, and L. Pino, Modeling Polymer Electrolyte Fuel Cells: an Innovative Approach, *J. Power Sources,* 2001, **101,** p 275-286
15. P. Costamagna, Transport Phenomena in Polymeric Membrane Fuel Cells, *Chem. Eng. Sci.,* 2001, **56,** p 323-332
16. R.F. Mann, C. John, Amphlett, Michael A.I. Hooper, Heidi M. Jensen, Brant A. Peppley, and Pierre R. Roberge, Development and Application of a Generalized Steady-State Electrochemical Model for a PEM Fuel Cell, *J. Power Sources,* 2000, **86,** p 173-180
17. M. Krumpelt, R. Kumar, and K.M. Myles, Fundamentals of Fuel Cell System in Integration, *J. Power Sources,* 1994, **49,** p 37-51
18. R. Cownden, M. Nahon, and M.A. Rosen, Modeling and Analysis of a Solid Polymer Fuel Cell System for Transportation Applications, Int. *J. Hydrogen Energy,* 2001, **26,** p 615-623
19. D.S. Watkins, K.W. Dircks, and D.G. Epp, Novel Fuel Cell Fluid Flow Field Plate, U.S. Patent 4 988 583 Jan 29, 1991
20. F. Barbir, J. Braun, and J. Neutzler, "Energy Partners Report 1999," Energy Partners Report 1999
21. A. Kumar and R.G. Reddy, "PEM Fuel Cell Bipolar Plate-Material Selection, Design And Integration," EPD Congress 2002, p 41-53
22. D. Thirumalai and R.E. White, Mathematical Modeling of Proton-Exchange-Membrane Fuel-Cell Stacks, *J. Electrochem. Soc.,* 1997, **144,** p 1717-1723
23. R. Ahluwalia, X. Wang, A. Rousseau, and R. Kumar, Fuel Economy of Hydrogen Fuel Cell Vehicles, *J. Power Sources,* 2004, **130,** p 192-201
24. D. Arthur Little, Inc. "Projected Automotive Fuel Cell Use in California," Contract No. 500-00-002 (WA 8), 2001